

TIME-RESOLVED MEASUREMENT AND SIMULATION OF A LONGITUDINAL SINGLE-BUNCH INSTABILITY AT THE MAX IV 3 GeV RING

M. Brosi*, Å. Andersson, J. Breunlin, F. Cullinan, and P. Fernandes Tavares
Lund University - MAX IV, Lund, Sweden

Abstract

The study and understanding of collective effects plays a vital role for fourth-generation light sources. These effects mostly need to be mitigated and controlled to achieve the design operational parameters. However, they can also be utilized to gain insights into the properties of the machine. While the 3 GeV storage ring at the MAX IV light source is running in multi-bunch mode during user operation, single-bunch operation is available in dedicated machine study shifts, providing the possibility to study collective effects at higher bunch currents. In such a current range an instability has been observed in the longitudinal plane. Above the threshold current of the instability a dynamic deformation of the longitudinal bunch profile and a strong increase in energy spread occurs. Dedicated measurements were conducted with multiple diagnostic tools such as time-resolved bunch profile measurements. First simulations of the observed effects were performed with a Vlasov-Fokker-Planck solver. This contribution presents measurement results and draws a comparison to the simulations.

INTRODUCTION

The interaction of a bunch with itself and its surroundings, which can be described by impedances, can lead to instabilities. Collective instabilities additionally depend on bunch properties like bunch charge, length or transverse dimensions. One prominent example is the microwave instability, a longitudinal, single-bunch, collective instability which leads to an increase of relative energy spread and dynamic deformations of the longitudinal bunch profile. It has been described numerous in the past (e.g., [1–3]) and is sometimes also referred to as turbulent bunch lengthening or sawtooth instability. It rarely leads to current loss and has been referred to as being “self-regulating”. In this contribution observations and simulations of bunch properties during a longitudinal instability are presented and compared to the expectations of the microwave instability.

MEASUREMENTS

The presented measurements were taken during dedicated machine study shifts at the 3 GeV ring. A single bunch was stored to, firstly, enable the usage of a bigger bunch current range unavailable in multi-bunch operation. And secondly to ensure that the observed dynamics originate from single bunch effects, with respect to the beam dynamics as well as the diagnostics. The optics were unchanged with respect to standard operations [4], while the main acceleration volt-

Table 1: Beam Parameters for Simulations

| Set | A | B |
|-----------------------------------|--------|--------|
| RF voltage / MV | 1.236 | 0.864 |
| Synchrotron freq. / kHz | 1.049 | 0.832 |
| Natural rel. energy spread / 1e-3 | 0.7898 | 0.7898 |
| Long. damping time / ms | 14.066 | 14.066 |
| Natural bunch length (rms) / ps | 37.2 | 44.6 |

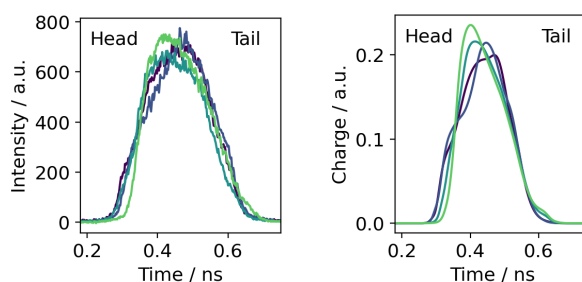


Figure 1: Measurement (left) and simulation (right) of individual bunch profiles for set A at 8 mA.

age was changed for the two presented measurement sets. All IDs were opened. Table 1 lists the parameters used for the simulation set A and B with the RF voltage and the synchrotron frequency taken during the measurements.

A streak cameras is set up at one of the optical diagnostic beam lines [5] of the 3 GeV ring. The Hamamatsu universal streak cameras of type C10910 [6] are equipped with a dual time-base extender. This enables measurements with a fast and slow time axis simultaneously, and can be used to measure the longitudinal bunch profile (e.g., Fig. 1) over different time scales ranging from multiple turns to several milliseconds within one image (e.g., Fig. 2a), resolving the temporal dynamics of the instability. For the presented bunch length a Gaussian fit was applied to the background corrected profiles to extract the standard deviation as bunch length.

The longitudinal spectrum was measured using the Dintel Bunch-by-Bunch system [7]. Fourier transforming a BPM sum signal gives the longitudinal motion spectrum of a selected bunch. Performing several measurements at different bunch currents results in spectrograms as shown in Fig. 3.

The energy spread is measured at two visible to near-UV diagnostic beam lines [5] using an interferometric techniques to determine the transverse beam sizes, allowing the calculation of both emittances and the energy spread. Due to the necessary integration time of the cameras the measured energy spread does not resolve the fast dynamics during the instability. It rather corresponds to a time average and mainly shows the current dependent changes.

* miriam.brosi@maxiv.lu.se

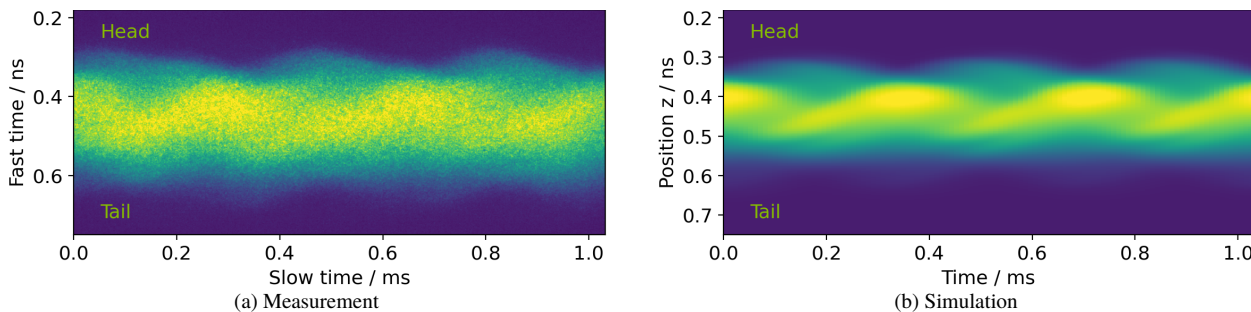


Figure 2: Measurement (a) and simulation (b) of the longitudinal bunch profile over 1 ms (≈ 1 synchrotron oscillation period) (set A at 8 mA). The dynamic changes of the profile (vert. axis) with time (hor. axis) are the result of the instability.

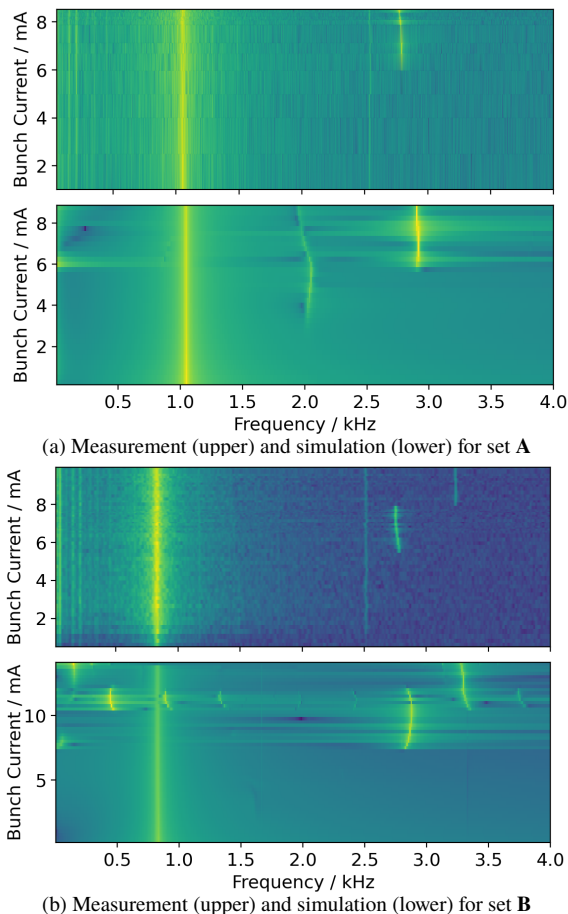


Figure 3: Spectrogram of long. center of mass movement (measured and simulated) for set A (a) and for set B (b).

SIMULATION

Simulations of the longitudinal dynamics were performed using the Vlasov-Fokker-Planck solver Inovesa [8]. The solver simulates purely the longitudinal phase space and operates on a grid representing the charge density. Solving the VFP equation for each time step, it simulates the temporal evolution of the charge density for a given bunch current including synchrotron motion, radiation damping and diffusion, as well as the influence of any longitudinal impedance provided. While Inovesa was mainly used to simulate the micro-bunching instability caused by the CSR-Impedance acting on short electron bunches (e.g., [9–11]), its design

was deliberately kept generic to allow the application to any longitudinal dynamic arising from an interaction describable by an impedance. For the presented simulations, a grid of 512 bins was chosen, covering a range from -12 to $+12 \sigma_0$ for the longitudinal as well as energy axis of the phase space.

As impedance model, a combination of a geometric and a resistive wall impedance was used. The geometric impedance was derived from GdfidL [12] simulations reaching up to a frequency of 30 GHz [13]. Different methods of extrapolation to the higher frequencies required by Inovesa were tested and the effect was found to be negligible.

The resistive wall contribution was calculated in ImpedanceWake2D [14], considering the multi-layer setup of the vacuum chamber with NEG coating. The calculated impedance ranges up to 100 THz. For the presented simulation, the re-binning for Inovesa results in a frequency resolution of 195 MHz and a maximal frequency of 200 GHz (or 139 MHz respective 286 GHz for set B).

RESULTS

The temporal changes in the profile show the deforming and turbulent nature of the instability (see Fig. 2). The bunch profile is far from Gaussian and continuously changing with a repeating pattern. For both measurement and simulation the pattern repeats approximately 3 times within 1 synchrotron period. The periodicity of this deformation is also visible in the longitudinal center of mass movement as shown in Fig. 3a, where for the higher currents a frequency component of ≈ 2.77 kHz in the measurement and ≈ 2.91 kHz in the simulation is present additionally to the synchrotron frequency of 1.05 kHz. This additional frequency stops for set A around 6 mA indicating the transition to a stable bunch. In the measured bunch length as function of bunch current in Fig. 4a an increase in fluctuation is observed for currents above 6–6.5 mA coinciding with the threshold observed in the center of mass movement. At the same time, the measured energy spread shows a stronger increase for currents above this threshold. The simulations show the threshold also at 6 mA by a significant increase in the energy spread as well as an onset of fluctuations of the bunch length. These observations correspond nicely to the expectations of the microwave instability to show a turbulent dynamics in the bunch length accompanied by an increase in energy spread above a certain threshold in bunch current.

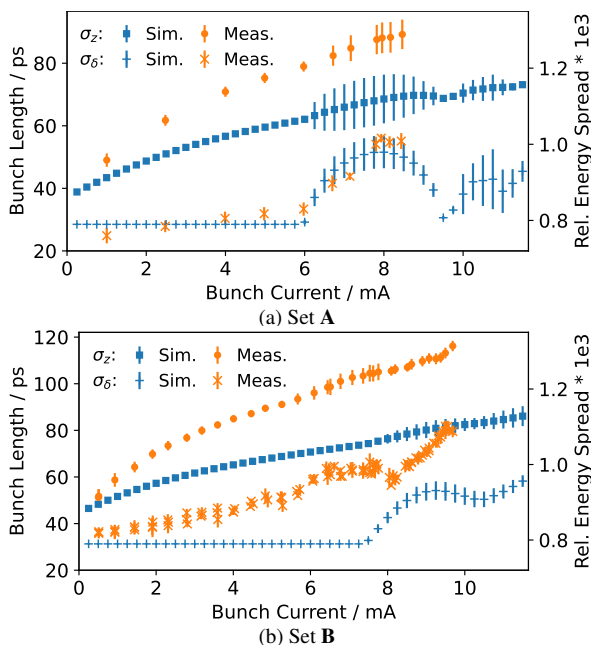


Figure 4: Bunch length σ_z and energy spread σ_δ measurements and simulations are shown for set **A** (a) and set **B** (b). The error bars on the bunch length, indicating the fluctuation, were multiplied by 2 (a) and 4 (b) to improve the visibility.

The increase in energy spread already below the threshold current might be caused by intrabeam scattering due to the low transverse emittances in the MAX IV 3 GeV ring [15, 16]. The simulation does not include the effects of IBS and shows a constant energy spread at the zero-current level as expected. Additionally, this could account for a part of the difference observed in bunch lengthening between simulation and measurement. Test measurements showed that it is possible to suppress the effect of IBS, and return the energy spread to the zero-current value, for lower currents, by increasing the vertical bunch size with an excitation.

Figure 4b shows similarly, for set **B**, a kink in the increase of the measured energy spread as a function of bunch current at the same current where the measured bunch length starts to experience fluctuations. This threshold current indicating the first onset of the instability differs for this case with ≈ 5.8 mA in the measurements and 7.5 mA in the simulations, hinting at a potentially insufficient impedance model.

While in set **A** (Fig. 4a) the measurement does not cover the current, where an intermediate decrease in energy spread occurs in the simulation (9.5 mA), measurement set **B** exhibits this local minimum (Fig. 4b). In Ref. [17], supported by energy spread measurements at the NSLS II ring, these local minima of the energy spread are interpreted as higher-order thresholds of the microwave instability showing fluctuation frequencies separated by approx. one synchrotron frequency. This change in oscillation frequency is visible in the measurement of set **B** (Fig. 3b) at the same current as the observed local minima in energy spread although, compared to [17], the separation is slightly less than one synchrotron frequency. In the corresponding simulation, the current at the frequency change also coincides with the dip

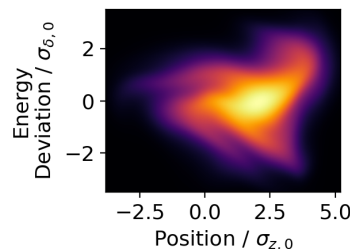


Figure 5: Simulated long phase space for set **A** at 8 mA.

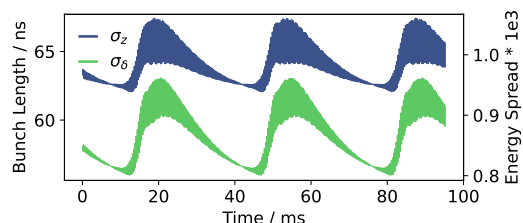


Figure 6: Simulated bunch length σ_z and energy spread σ_δ as function of time at 10 mA for set **A**.

in simulated energy spread (Fig. 4b) but deviates, similar to the threshold current for this set, from the measurement. Additionally, the frequencies overlap for a short intermediate current range.

These fast fluctuations of the center of mass and the bunch profile in the order of small multiples of the synchrotron frequency arise from the rotation and shape of the charge distribution in the phase space. This is supported by the simulated charge distribution (Fig. 5) showing an approximately three-fold symmetry. A similar symmetry was early on observed for some of the simulation parameters in Ref. [3]. Much slower, but stronger and sawtooth-shaped fluctuations of bunch length and energy spread are visible in the simulated bunch at currents higher than the ones covered by the measurement (see Fig. 6). Such fluctuations were already observed in the '90s (e.g., [2, 18]) giving the microwave instability also the name sawtooth instability. While the dynamics were often accompanied by microwave emissions, these are expected to be suppressed at the MAX IV 3 GeV ring due to the small vacuum chamber aperture.

SUMMARY

A longitudinal single bunch instability can be observed in single bunch operation at the MAX IV 3 GeV storage ring at bunch currents higher than the design value. Time-resolved measurements of the longitudinal bunch profile show a dynamic deformation above a threshold current, supported further by measurements of an increase in energy spread and additional fluctuations on the longitudinal beam position spectrum. Simulations with a Vlasov-Fokker-Plank solver considering the geometric and resistive wall impedance qualitatively reproduce the same dynamic. The observed characteristics correspond well to observations at other light sources and predictions for the microwave instability.

ACKNOWLEDGEMENTS

The authors would like to thank Patrick Schreiber for the extensive support with the Inovesa simulations.

REFERENCES

- [1] F. J. Sacherer, “Bunch Lengthening and Microwave Instability”, *IEEE Trans. Nucl. Sci.*, vol. 24, no. 3, pp. 1393–1395, June 1977. doi:10.1109/TNS.1977.4328955
- [2] P. Krejcik *et al.*, “High Intensity Bunch Length Instabilities in the SLC Damping Rings”, in *Proc. PAC’93*, Washington D.C., USA, Mar. 1993, pp. 3240–3243, http://accelconf.web.cern.ch/AccelConf/p93/PDF/PAC1993_3240.PDF
- [3] Alban Mosnier, “Microwave instability in electron storage rings”, *Nucl. Instrum. Methods Phys. Res., Sect. A*, vol. 438, 1999, pp. 225–245. doi:10.1016/S0168-9002(99)00832-3
- [4] P. F. Tavares *et al.*, “Commissioning and first-year operational results of the MAX IV 3 GeV ring”, *J. Synchrotron Radiat.*, vol. 25, 2018. doi:10.1107/S1600577518008111
- [5] J. Breunlin and Å. Andersson, “Emittance Diagnostics at the Max Iv 3 GeV Storage Ring”, in *Proc. IPAC’16*, Busan, Korea, May 2016, pp. 2908–2910. doi:10.18429/JACoW-IPAC2016-WEPOW034
- [6] Hamamatsu, Streak Camera C10910, <https://www.hamamatsu.com/eu/en/product/photometry-systems/streak-camera/universal-streak-camera/C10910-05.html>
- [7] Dimtel, Inc., <https://www.dimtel.com>
- [8] P. Schönfeldt *et al.*, Inovesa/Inovesa: The ones (v1.1.1), 2021. doi:10.5281/zenodo.4446191
- [9] M. Brosi, “Overview of the Micro-Bunching Instability in Electron Storage Rings and Evolving Diagnostics”, in *Proc. IPAC’21*, Campinas, Brazil, May 2021, pp. 3686–3691. doi:10.18429/JACoW-IPAC2021-THXA02
- [10] T. Boltz *et al.*, “Studies of Longitudinal Dynamics in the Micro-Bunching Instability Using Machine Learning”, in *Proc. IPAC’18*, Vancouver, Canada, Apr.-May 2018, pp. 3277–3279. doi:10.18429/JACoW-IPAC2018-THPAK030
- [11] P. Schreiber *et al.*, “Effect of Negative Momentum Compaction Operation on the Current-Dependent Bunch Length”, in *Proc. IPAC’21*, Campinas, Brazil, May 2021, pp. 2786–2789. doi:10.18429/JACoW-IPAC2021-WEPA083
- [12] W. Bruns, “The GdfidL Electromagnetic Field Simulator”, <http://www.gdfidl.de>
- [13] M. Klein, R. Nagaoka, G. Skripka, P. F. Tavares, and E. J. Wal-lén, “Study of Collective Beam Instabilities for the MAX IV 3 GeV Ring”, in *Proc. IPAC’13*, Shanghai, China, May 2013, paper TUPWA005, pp. 1730–1732, <https://accelconf.web.cern.ch/ipac2013/papers/tupwa005.pdf>
- [14] N. Mounet *et al.*, ImpedanceWake2D, CERN, Geneva, <https://gitlab.cern.ch/IRIS/IW2D>
- [15] M. Eriksson *et al.*, “Commissioning of the MAX IV Light Source”, in *Proc. IPAC’16*, Busan, Korea, May 2016, pp. 11–15. doi:10.18429/JACoW-IPAC2016-MOYAA01
- [16] P. F. Tavares *et al.*, “Status of the MAX IV Accelerators”, in *Proc. IPAC’19*, Melbourne, Australia, May 2019, pp. 1185–1190. doi:10.18429/JACoW-IPAC2019-TUYPLM3
- [17] A. Blednykh *et al.*, “New aspects of longitudinal instabilities in electron storage rings”, *Sci. Rep.*, vol. 8, p. 11918, 2018. doi:10.1038/s41598-018-30306-y
- [18] U. Arp *et al.*, “Spontaneous coherent microwave emission and the sawtooth instability in a compact storage ring”, *Phys. Rev. Accel. Beams*, vol. 4, p.054401, 2001. doi:10.1103/PhysRevSTAB.4.054401